Supporting Information

Visualization of autophagy progression by Red-Green-Blue autophagy sensor

Heejung Kim[1,2], Hyunbin Kim[1,3], Jaesik Choi[4], Kyung-Soo Inn[2*] and Jihye Seong[1-3*]

[1]Convergence Research Center for Diagnosis Treatment Care of Dementia, Brain Science Institute, Korea Institute of Science and Technology (KIST), Seoul, South Korea

[2]Department of Converging Science and Technology, Kyung Hee University, Seoul, South Korea

[3]Division of Bio-Medical Science & Technology, KIST School, Korea University of Science and Technology, Seoul, South Korea

[4]Graduate School of Artificial Intelligence, Korea Advanced Institute of Science and Technology (KAIST), Daejeon, Republic of Korea

Name	λ_{ex}	λ_{em}	Stokes	EC	QY	Brightness	pKa	Aggregation
Sirius	355	424	69	15,000	0.24	3.6	3	m
mTagBFP2	399	454	55	50,600	0.64	32.38	2.7	m
mTagBFP	402	457	55	52,000	0.63	32.76	2.7	m
mBlueberry2	402	467	65	51,000	0.48	24.48	2.5	m
mTurquoise2	434	474	40	30,000	0.93	27.9	3.1	m
SCFP2	434	474	40	29,000	0.41	11.89	3.5	m
Aquamarine	430	474	44	26,000	0.89	23.14	3.3	m
mCerulean3	433	475	42	40,000	0.87	34.8	3.2	m
SCFP1	434	477	43	29,000	0.24	6.96	3.5	m

Figure S1. *In vitro* characterization of various fluorescent proteins

Physicochemical properties of different blue fluorescent proteins: spectral profiles, extinction coefficient (EC), quantum yield (QY), brightness, pKa and aggregation. The information was achieved from FPbase [1].

Name	λ_{ex}	λ_{em}	Stokes	EC	QY	Brightness	pKa	Aggregation
mOrange	548	562	14	71,000	0.69	48.99	6.5	m
mOrange2	549	565	16	58,000	0.6	34.8	6.5	m
mApple	568	592	24	75,000	0.49	36.75	6.5	m
PAmCherry1 (On)	564	595	31	18,000	0.46	8.28	6.3	m
PAmCherry2 (On)	570	596	26	24,000	0.53	12.72	6.2	m
PAmCherry3 (On)	570	596	26	21,000	0.24	5.04	6.2	m
mGinger2	578	631	53	36,000	0.04	1.44	6.5	m
mKate	588	635	47	45,000	0.33	14.85	6.2	m
mGrape2	605	636	31	33,000	0.03	0.99	6.3	m
mRouge	600	637	37	43,000	0.02	0.86	6.1	m
mNeptune2.5	599	643	44	95,000	0.24	22.8	5.8	m
Neptune	600	650	50	72,000	0.18	12.96	5.8	d
mNeptune2	599	651	52	89,000	0.24	21.36	6.3	m
mMaroon1	609	657	48	80,000	0.11	8.8	6.2	m
mNeptune684	604	684	80	39,000	0.03	1.17	6.5	m

Figure S2. *In vitro* characterization of various fluorescent proteins

Physicochemical properties of orange to far-red fluorescent proteins: spectral profiles, extinction coefficient (EC), quantum yield (QY), brightness, pKa and aggregation. The information was achieved from FPbase [1].

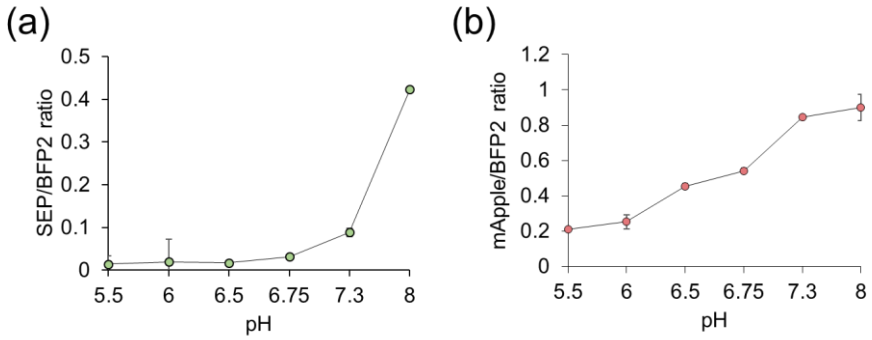

Figure S3. Different pH sensitivity of SEP and mApple of RGB-LC3 in HEK293A cells.
(a-b) The intensity ratios of SEP/mTagBFP2 (a) and mApple/mTagBFP2 (b) of RGB-LC3 sensor expressed in HEK cells under different pH conditions. The representative images were shown in Figure 3c. Data indicate the mean value ± s.d. (n=10).

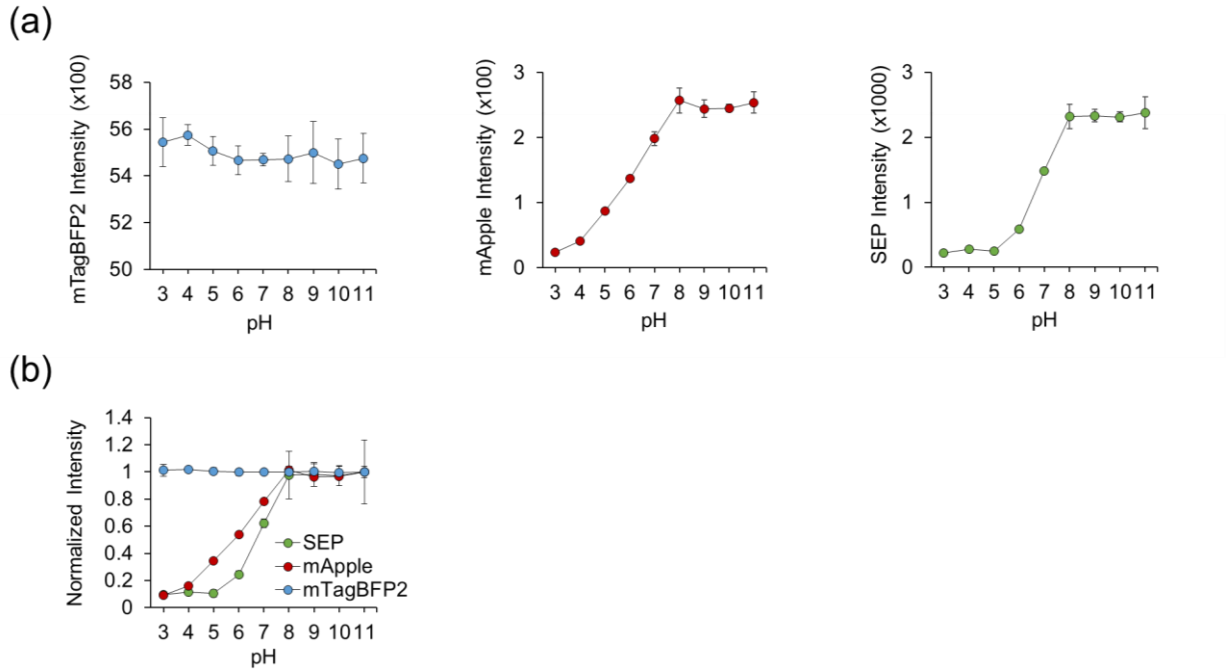

Figure S4. The pH titration curves of mTagBFP2, mApple and SEP of the purified RGB-LC3.

(a) The pH titration curves for the fluorescent intensity of mTagBFP2 (n=5), mApple (n=5), and SEP (n=5) in the purified full length RGB-LC3. (b) The merged graph displaying different pH senstivities of mTagBFP2, mApple and SEP. Data indicate the mean value ± s.e.m.

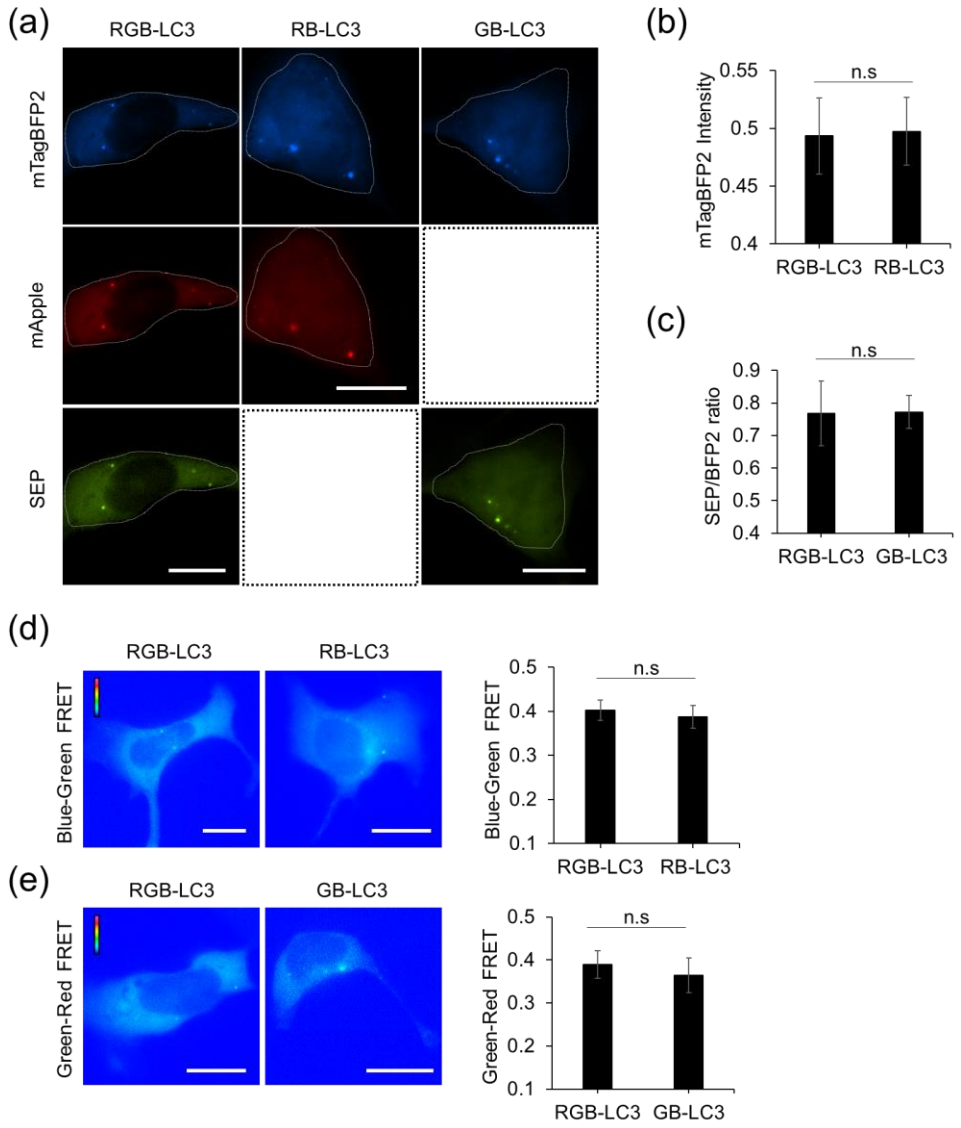

Figure S5. No FRET was detected between the FPs of RGB-LC3 in phagophores of HEK293A cells.

(a-c) Representative images of mTagBFP2, mApple and SEP in the HEK293A cells expressing RGB-LC3, RB-LC3 or GB-LC3 after the treatment with 200 nM rapamycin and 50 μM 3-MA for 6 hours (a). Scale bar, 20 μm. No difference was observed in (b) the mTagBFP2 intensity in the phagophores of the cells expressing RGB-LC3 and RB-LC3, and (c) the SEP/mTagBFP2 ratio in the phagophores of the cells expressing RGB-LC3 and GB-LC3. Data indicate the mean value ± s.e.m. (N=10). (d-e) Representative images of Green-Red FRET (excitation filter 482DF40, emission filter 641DF40) in the cells expressing RGB-LC3 or RB-LC3 (d) and Blue-Green FRET (excitation filter 377DF40, emission filter 536DF40) in the cells expressing RGB-LC3 or GB-LC3 (e) after the treatment with 200 nM rapamycin and 50 μM 3-MA for 6 hours

(a). Scale bar, 20 μm. No difference was observed in (d) the Green-Red FRET level in the phagophores of the cells expressing RGB-LC3 and RB-LC3, and (e) the Blue-Green FRET level in the phagophores of the cells expressing RGB-LC3 and GB-LC3. Data indicate the mean value ± s.e.m. (N=10).

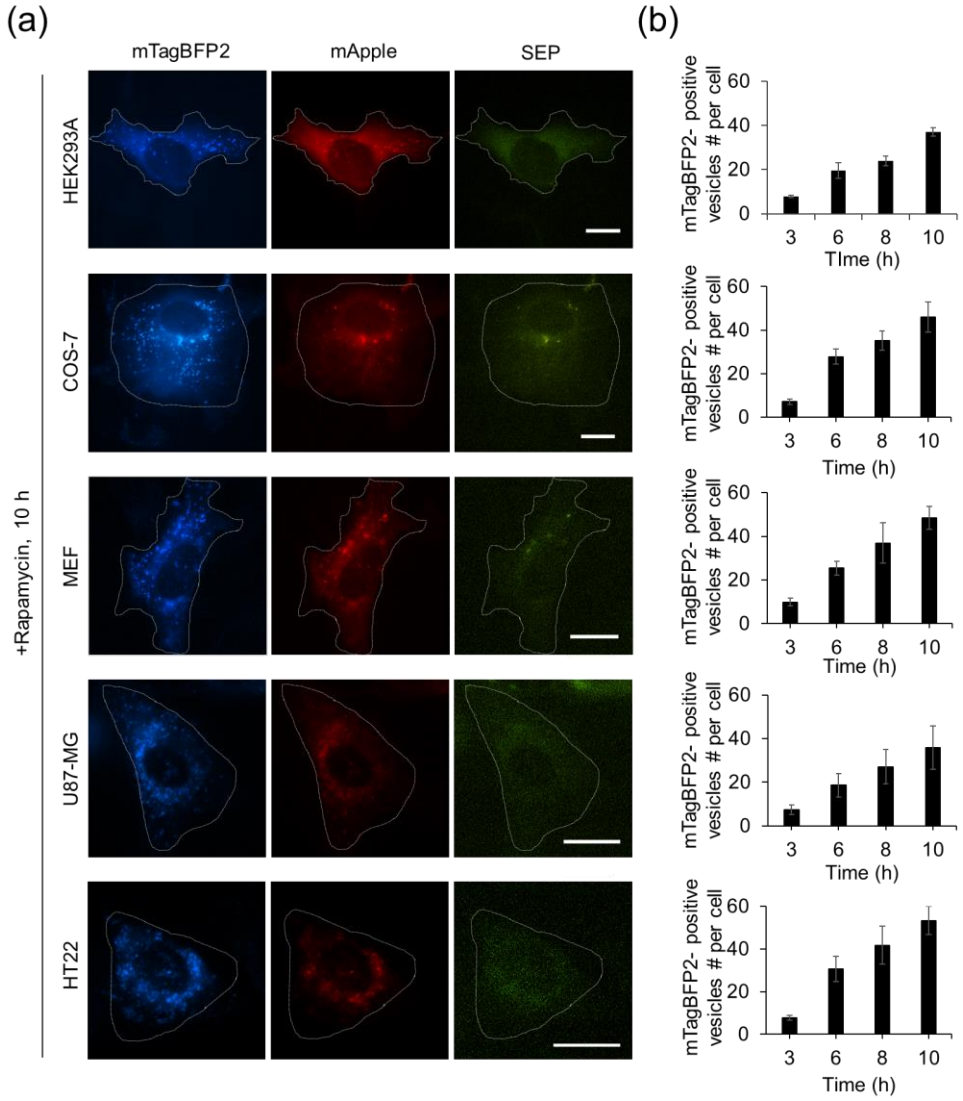

Figure S6. RGB-LC3 can monitor the autophagy progression in different cell types.

(a) Representative images of mTagBFP2, mApple and SEP of RGB-LC3 expressed in the indicated cell lines after the treatment of 200 nM rapamycin for 10 hours. Scale bars, 20 μm. (b) Total numbers of mTagBFP2-positive vesicles per cell in different cell lines after the treatment of rapamycin for indicated times. Data indicate the mean values ± s.e.m. (N=10 cells).

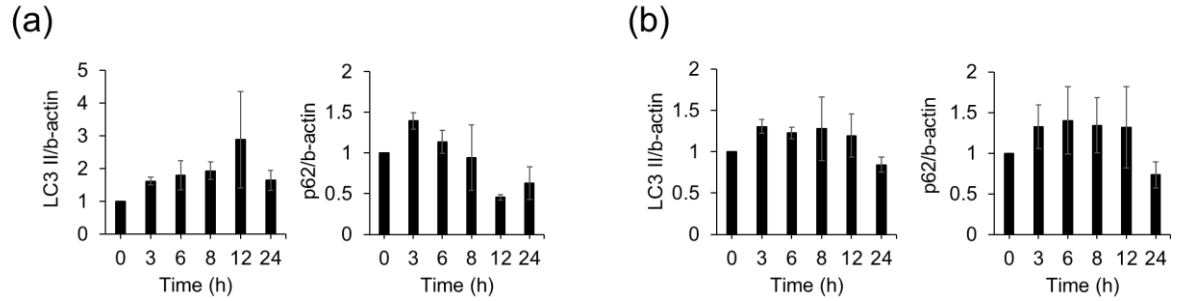

Figure S7. The RGB-LC3 sensor does not interfere endogenous autophagic flux

(**a**-**b**) The expression levels of LC3-I, II and p62 in HEK293A cells without **(a)** or with the expression of RGB-LC3 sensor **(b)** after the treatment of 200 nM rapamycin at indicated times. The relative levels of LC3-II and p62 normalized by β-actin were displayed (n=3).

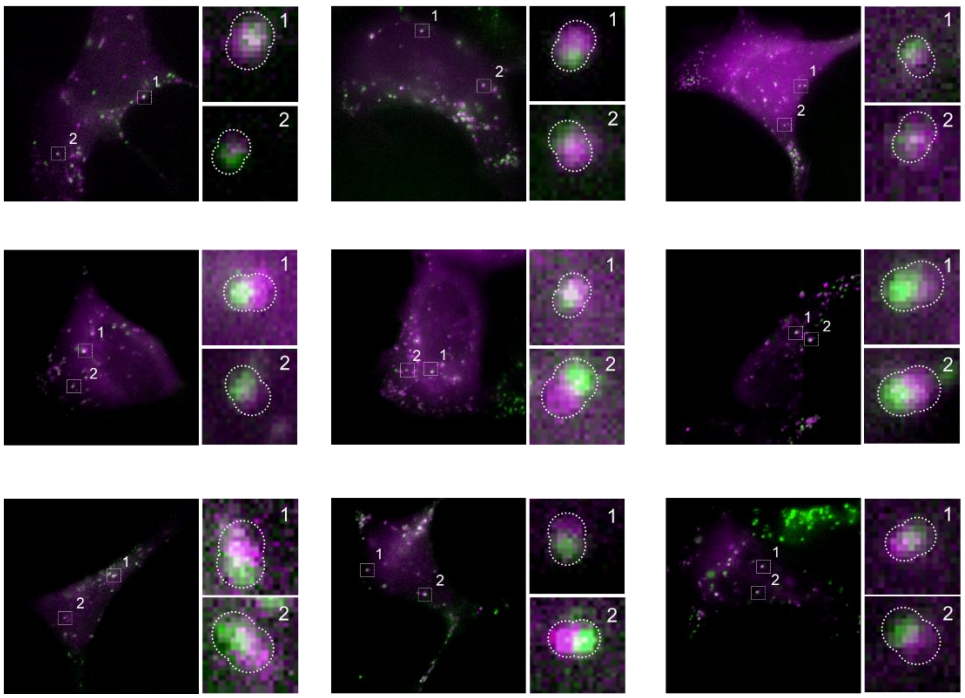

Figure S8. The fusion stage of autophagosomes and lysosomes. The HEK293A cells expressing RB-LC3 and LysoTracker (50 nM) were treated with 200 nM rapamycin for 8 hours. The mTagBFP2-positive autophagic vesicles (magenta) in contact with LysoTracker (green) of the boxes in left panels were displayed with a high magnification in the right panels.

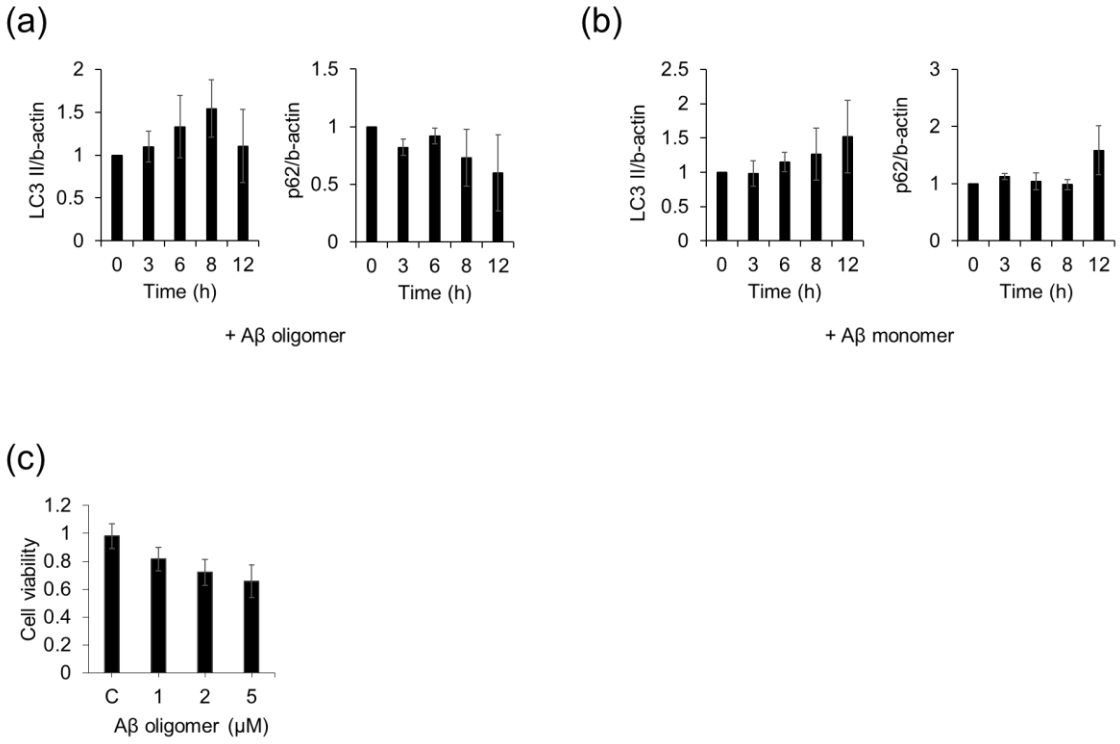

Figure S9. Different effects of Aβ monomer and oligomer on autophagy flux.

(a-b) The western blot results in Fig. 6F-G were quantified. The relative levels of LC3-II and p62 were normalized by β-actin in HT22 cells after the treatment of oligomeric Aβ **(a)** or monomeric Aβ **(b)** for indicated times (n=3). **(c)** The viability of the HT22 cells treated by different concentrations of oligomeric Aβ for 24 hr.

Reference

(1) Lambert, T. J. FPbase: a community-editable fluorescent protein database. *Nat Methods* **2019,** *16* (4), 277-278, DOI: 10.1038/s41592-019-0352-8.